HHS Public Access

Author manuscript

Magn Reson Med. Author manuscript; available in PMC 2017 December 01.

Published in final edited form as:

Magn Reson Med. 2016 December ; 76(6): 1764–1774. doi:10.1002/mrm.26076.

Phase-cycled simultaneous multi-slice balanced SSFP imaging with CAIPIRINHA for efficient banding reduction

Yi Wang[1], **Xingfeng Shao**[1], **Thomas Martin**[1], **Steen Moeller**[2], **Essa Yacoub**[2], and **Danny JJ Wang**[1,*]

[1]Laboratory of FMRI Technology (LOFT), Department of Neurology, University of California Los Angeles, Los Angeles, CA 90095, United States

[2]Center of Magnetic Resonance Research, University of Minnesota, Minneapolis, MN 55455, United States

Abstract

Purpose—To present a time-efficient technique for banding reduction in balanced steady-state free precession (bSSFP) imaging by utilizing phase-cycled simultaneous multi-slice (SMS) acquisition with CAIPIRINHA (controlled aliasing in parallel imaging results in higher acceleration).

Theory—The proposed technique exploits the inherent phase modulation of SMS imaging with CAIPIRINHA to acquire multiple phase-cycled images, which can be combined for efficient banding reduction within the same scan time of a single-band bSSFP scan.

Methods—Bloch equation simulation, phantom and *in vivo* brain, abdominal and cardiac imaging experiments were performed on healthy volunteers at 3T using multi-channel head and body array coils with SMS acceleration factors of two to four. The performance of banding reduction was quantitatively evaluated based on the percent ripple of signal distribution and signal-to-noise ratio (SNR) efficiency in both phantom and human studies.

Results—The banding artifact was successfully removed or suppressed using phase-cycled SMS bSSFP imaging across SMS factors of two to four. The performance of banding reduction improved with higher SMS factors along with increased SNR efficiency.

Conclusion—Phase-cycled SMS bSSFP with CAIPIRINHA is a promising technique for efficient band reduction in bSSFP without prolonged scan time. Further evaluation of this technique in clinical applications is warranted.

Keywords

Simultaneous Multi-Slice (SMS); controlled aliasing in parallel imaging results in higher acceleration (CAIPIRINHA); balanced steady-state free precession (bSSFP); banding reduction

[*]Corresponding Author: Danny JJ Wang, PhD, MSCE, Department of Neurology, University of California Los Angeles, 660 Charles E Young Dr South, Los Angeles, CA 90095, USA, jwang71@gmail.com, 310-983-3667 (phone) 310-794-7406 (fax).

Introduction

Balanced steady state free precession (bSSFP) is a widely used fast imaging technique characterized by its high SNR efficiency and the T_2/T_1 contrast (1-3). Due to the unique signal and contrast behavior, as well as the fast imaging time, bSSFP has been of interest to a wide range of clinical applications including cardiac imaging (4), abdominal imaging (5), angiography (6), functional MRI (7), and musculoskeletal imaging (8). However, a major limitation of bSSFP lies in its sensitivity to the B_0 field inhomogeneity resulting in the banding artifact—signal voids at certain off-resonance frequencies.

Techniques have been proposed to alleviate or remove the banding artifact (9-12). One of the common approaches is to perform multiple acquisitions with different RF phase cycling, i.e., different phase increment between sequential RF pulses. Taking advantage of the 2π-periodic profiles of the bSSFP signal, multiple phase-cycled images with spatially shifted banding artifact can thus be combined to form a composite image with reduced banding. As demonstrated by Bangerter *et al.* (9), the performance of the banding artifact reduction is improved as the number of phase-cycled images increases. This inevitably lengthens the total acquisition time, discounting the inherent benefit of the fast imaging nature of bSSFP and making it susceptible to motion between the measurements. To overcome these drawbacks, dynamically phase-cycled radial bSSFP (DYPR-SSFP) acquisition was recently proposed where each radial projection was acquired with a small phase increment, and a banding-free image can be attained from one single-shot measurement (13). However DYPR-SSFP requires a large number of projections and a relatively lengthy magnetization preparation.

The simultaneous multi-slice (SMS) excitation with the controlled aliasing in parallel imaging results in higher acceleration (CAIPIRINHA) technique has recently been applied for accelerated bSSFP imaging (14,15). The technique allows multiple imaging slices to be excited simultaneously by using multiband (MB) composite RF pulses, followed by separation of aliased imaging slices using the spatial sensitivity profile of the phased array coil (16,17). To reduce the noise amplification, the CAIPIRINHA (18) technique was applied such that the aliased slices are shifted relative to each other by modulating the phase of the MB excitation pulses. However, modulating the phase of the MB excitation pulses in bSSFP results in not only shift of the aliased imaging slices in space, but also shift in the off-resonance profiles of bSSFP signals. For instance, an imaging slice that is FOV/2 shifted in space is simultaneously shifted in its off-resonance profile by π. In the work of Stäb *et al.* (15), a MB factor of two was realized by shifting the center frequency to yield an off-resonance angle of $\pm\pi/2$ for the two simultaneously excited imaging slices respectively, as a tradeoff between achieving SMS acceleration and minimizing banding artifacts.

The purpose of this study is to present a new technique for banding artifact reduction by utilizing the shifted off-resonance profile from the CAIPIRINHA shifted SMS (CAIPI-SMS) bSSFP imaging. Hence, each un-aliased imaging slice is subject to different off-resonance behavior similar to that of the phase-cycled single-band bSSFP, whereas the total scan time is drastically reduced due to the SMS acceleration. Simulations were performed to predict the behavior of the SMS bSSFP signal with varying number of ramp up preparation pulses.

In addition, the proposed phase-cycled CAIPI-SMS bSSFP approach was compared with the conventional multiple-acquisition phase-cycled bSSFP in a phantom study. Finally, the feasibility of the presented technique for time-efficient banding reduction was demonstrated with *in vivo* brain, abdominal and cardiac imaging.

Theory

The proposed concept of phase-cycled CAIPI-SMS bSSFP exploits the inherent phase modulation in CAIPIRINHA. Using a simple one-dimensional example, the signal intensity of P simultaneously excited slices $\rho(y)_{\mathrm{CAIPI}}$ can be expressed as (15):

$$\rho(y)_{\mathrm{CAIPI}}=\sum_{m=-N/2}^{N/2-1}\left(\sum_{j=1}^{P}S_j(m\Delta k)\bullet e^{i\phi_j(m)}\right)\times e^{im\Delta ky}=\sum_{j=1}^{P}\rho_j(y+\Delta y_j) \quad [1]$$

where S_j is the k-space signal of slice j, $\phi_j(m)$ denotes the phase of the m-th pulse for slice j. As the result of linear phase modulation, the image of slice j is shifted by Δy_j along the phase encoding direction. The CAIPIRINHA technique was originally developed for gradient echo sequences. For bSSFP imaging, however, the phase modulation of CAIPIRINHA also yields frequency shift on the off-resonance profile. Therefore, the CAIPI-SMS bSSFP signal $\rho(y, \omega_0)_{\mathrm{CAIPI\text{-}bSSFP}}$ should be expressed as a function of both the spatial location y and excitation frequency ω_0,

$$\rho(y,\omega_0)_{\mathrm{CAIPI-bSSFP}}=\sum_{m=-N/2}^{N/2-1}\left(\sum_{j=1}^{P}S_j(m\Delta k,\rho_0)\bullet e^{i\phi_j(m)}\right)\times e^{im\Delta ky}=\sum_{j=1}^{P}\rho_j(y+\Delta y_j,\omega_0+\Delta\omega_j)$$

[2]

where the k-space signal S_j is a function of both k_y and ω_0. Here we propose a linear phase modulation as $\phi_j(m)=2\pi jm/p$, and the frequency shift in the off-resonance profile of slice j becomes

$$\Delta\omega_j=\frac{j}{\mathrm{TR}\bullet P}\ j=1,\ldots,\mathrm{P} \quad [3]$$

and the FOV shift of slice j is

$$\Delta y_j=\frac{j\bullet \mathrm{FOV}}{P}\ j=1,\ldots,\mathrm{P} \quad [4]$$

Using the proposed CAIPI-SMS bSSFP technique, simultaneously excited slices are evenly shifted in both space and off-resonance profile.

Differing from previous work on SMS bSSFP (14,15) where slice acceleration is the sole purpose, multiple imaging slices are acquired in the presented technique, yet each slice is excited multiple times by the MB composite pulse with different phase cycling (or shifts in off-resonance profile) using the CAIPIRINHA technique. Subsequently, multiple phase-cycled images with evenly shifted off-resonance profiles are attained at each slice location that can be combined to reduce banding artifacts. The number of different phase-cycled images for banding reduction N is equivalent to the SMS acceleration factor. Excluding the time for the reference scan for encoding the coil sensitivities, the imaging time for such a scan would be identical to that of a standard single-band bSSFP acquisition, yet the latter one is prone to banding artifacts.

For illustration purposes, an SMS factor of three with a FOV/3 shift is illustrated in Fig. 1. Three slices are excited simultaneously with a spatial shift of FOV/3 (red), 0 (blue) and –FOV/3 (green) along the phase encoding direction. This results in a $2\pi/3$, 0, and $-2\pi/3$ shift in their off-resonance profiles, respectively, as shown in Fig. 1(d). The same strategy can be applied for other SMS acceleration factors. As schematically illustrated in Fig. 1(a–c), the phase-cycled CAIPI-SMS bSSFP technique can be progressively implemented in three different schemes:

1. Sequential CAIPI-SMS imaging with repeated phase cycling

The most straightforward implementation is to sequentially acquire SMS slices from superior to inferior or *vice versa*, as shown in Fig 1(a). The center slices will have a complete set of phase-cycled images with shifted off-resonance profiles, which can then be combined for banding reduction. However, the shortcomings of this technique include: a) incomplete phase cycling for the boundary slices; and b) potentially high *g*-factor for small inter-slice gaps.

2. CAIPI-SMS imaging with temporally modulated phase cycling

In order to avoid the incomplete phase cycling of the boundary slices, CAIPI-SMS can be implemented at the same slice positions multiple times with temporally modulated phase cycling, as shown in Fig. 1(b). Note the modulated phase cycling is carried out in time, in addition to the CAIPIRINHA phase modulation for SMS imaging. Although the efficiency is improved by acquiring full sets of phase-cycled images for all the imaging slices, this method is still limited by potentially high *g*-factor for small inter-slice gaps.

3. Interleaved CAIPI-SMS imaging with temporally modulated phase cycling

The interleaved CAIPI-SMS imaging with modulated phase cycling is identical to the former scheme, except that MB slices are acquired in an interleaved fashion with a larger inter-slice gap, as depicted in Fig. 1(c). This approach is advantageous for dense multi-slice imaging to cover a large imaging volume, without being limited by the potentially high *g*-factor due to small inter-slice gaps as shown in scheme 1 and 2.

To summarize, the purpose of the RF phase-cycling in the CAIPI-SMS bSSFP are two folds: a) to generate the relative spatial shift in between the simultaneously excited imaging slices to reduce the *g*-factor, and hence, the noise amplification in the parallel image reconstruction; and b) to create the multiple phase-cycled images that can be combined for banding reduction. Compared to the conventional approach with separate acquisitions of each individual phase-cycled image, the proposed SMS bSSFP with CAIPIRINHA technique is more efficient since all the phase-cycled images required for banding reduction are acquired within the same imaging time as a standard bSSFP scan.

Methods

Simulations

Bloch equation simulation was performed to study the behavior of the CAIPI-SMS bSSFP signal using custom MATLAB programs (The MathWorks, Natick, MA). The effect of the number of ramp up preparation pulses on SMS bSSFP signals was investigated. The simulation was performed with the following parameters: TR/TE=4.2/2.1 ms, T_1=1100 ms, T_2=100 ms, flip angle (FA)=30°, SMS factor=2, 3, and 4, and the number of ramp up pulses=24 and 48. During the magnetization preparation, the identical composite MB excitation pulses as those during CAIPI-SMS bSSFP scans were applied with a linear ramp up of FA.

Phantom imaging

The FBIRN agarose gel phantom (19) with T_1 and T_2 values mimicking those of brain tissue were imaged on a 3T Siemens Prisma (Erlangen, Germany) scanner with a 32-channel head coil. A small piece of paper clip was placed on the surface of the gel phantom to intentionally create B_0 field inhomogeneity and banding artifacts on bSSFP images. A total of 12 phase-cycled slices were acquired using the three different CAIPI-SMS bSSFP schemes as proposed in the Theory section. The positions of the 12 imaging slices were identical across all the phantom experiments: SMS acceleration factors of 2 (with FOV/2 shift), 3 (with FOV/3 shift) and 4 (with FOV/4 shift). The MB inter-slice gap for scheme 1 and 2 were both 20 mm. For scheme 3, larger MB inter-slice gaps of 90, 60 and 45 mm were selected for the SMS factor of 2, 3 and 4, respectively.

For comparison, single-band phase-cycled bSSFP scans were performed with multiple acquisitions (N=2, 3 and 4). These single-band bSSFP scans simultaneously served as the reference scan to encode coil sensitivities for the CAIPI-SMS bSSFP scans with acceleration factors of 2, 3 and 4, respectively. The rest of the common imaging parameters were: FOV=256×256 mm^2, matrix size=192×192, slice thickness=5 mm, TR/TE=4.06/2.03 ms, FA=30°, bandwidth=555 Hz/Px, and phase encoding direction L–R. The image acquisition time for each slice was 974 ms. The MB excitation pulse had a *sinc* pulse shape with duration of 1000 μs. The same MB pulses were applied in the *in vivo* brain and abdominal imaging experiments.

In vivo imaging

All the *in vivo* experiments were performed on a 3T Siemens Prisma system, according to a protocol approved by the local Ethics Committee and written informed consent was obtained from all subjects. Three healthy participants (age = 23±2 years, 2 female) were recruited for brain imaging using a 32-channel head receiver coil. Another healthy participant (age=23 years, male) underwent abdominal and cardiac study using an 18-channel body matrix receiver coil and 12-channel spinal array receiver coil. The detailed imaging protocols are listed below:

Brain imaging—Using the same imaging protocol and parameters as the phantom study, 12 axial slices were acquired on the brain using both CAIPI-SMS and the conventional multiple-acquisition phase-cycled bSSFP sequences. Further, the effect of the ramp up preparation pulses was investigated (24 and 48 pulses). Additionally, in order to demonstrate the capability of the proposed CAIPI-SMS bSSFP technique for a full-volume multi-slice imaging, 24 axial slices without inter-slice gap were acquired using scheme 3 (Fig. 1(c)) to cover the whole brain. The imaging parameters were: SMS factor=4, CAIPIRINHA slice shift=FOV/4, MB acquisitions=6, and the MB inter-slice gap=30 mm. The total imaging time for such a volumetric bSSFP acquisition was 47 sec.

Abdominal imaging—Using a CAIPI-SMS bSSFP sequence with temporally modulated phase cycling (scheme 2, Fig. 1(b)), three axial slices were simultaneously acquired in a 9 sec breath-hold scan with an SMS acceleration factor of 3 and a FOV/3 slice shift (or 3 RF phase cycling). The imaging parameters for abdominal imaging were: FOV=380×380 mm^2, matrix size=320×320, slice thickness=5 mm, spatial resolution=1.2×1.2×5 mm^3, inter-slice gap=45 mm, TR/TE=3.64/1.82 ms, FA=19°, bandwidth=558 Hz/Px, measurements=3, and phase encoding direction A–P. The 9 sec image acquisition time included a dummy scan (an option that comes with the vender sequence) and a 150 ms dead time in between the slice acquisitions. The total scan time for abdominal imaging can be further reduced to ~4 sec by removing the dead time and the dummy scan without affecting the performance of SSFP banding reduction.

Cardiac imaging—Three short-axis cardiac images were simultaneously acquired using an ECG triggered breath-hold CAIPI-SMS bSSFP scan (scheme 2, Fig. 1(b)), with an SMS acceleration factor of 3 and a FOV/3 slice shift. The imaging parameters for cardiac imaging were: FOV=320×240 mm^2, matrix size=160×122, slice thickness=5mm, nominal spatial resolution=2×2×5 mm^3, inter-slice gap=25mm, partial Fourier=6/8, readout asymmetric echo allowed, TR/TE=2.6/1.09 ms, FA=51°, and bandwidth=800 Hz/Px. The acquired readout and phase encoding steps were 126 and 92, respectively. Images were acquired during the diastolic phase with an ECG trigger delay of 500 ms and an image acquisition window of around 350 ms. RF duration was shortened to 600 μs when RF mode was selected as ‘Fast’ during cardiac imaging.

Quantitative analysis

All the aliased MB slices were reconstructed using the slice-GRAPPA (20) algorithm with a kernel size of 3×3 (21). The resulting phase-cycled images were combined using both

maximum intensity and sum of squares algorithms. For cardiac imaging, we also performed non-rigid image registration using Advanced Normalization Tools (ANTs) to correct for motion between temporally modulated phase-cycled acquisitions before image combination to reduce banding artifacts.

To evaluate the effect of various SMS acceleration factors on banding reduction, both the percent ripple and the spatial signal-to-noise ratio (SNR) efficiency within the banding artifact affected regions, e.g. orbitofrontal cortex in brain images, were measured for combined images across all the SMS acceleration factors. A region-of-interest (ROI) was hand drawn in the orbitofrontal cortex of each subject. The percent ripple (9) defined in Eq. [5] provides a quantitative measure of the performance of various combination techniques for bSSFP banding artifact reduction:

$$\%\,\text{ripple}=100\times\frac{S_{\max}-S_{\min}}{S_{\text{mean}}} \quad [5]$$

For the calculation of spatial SNR, the noise variance was determined by the mean of the standard deviation of the image intensity from background ROIs of the corresponding SMS reconstructed images. Since the imaging acquisition time for each slice using phase-cycled CAIPI-SMS method is identical to that of standard bSSFP readout, the SNR efficiency η (9,22) can be estimated as:

$$\eta=100\times\frac{\text{SNR}}{g\cdot\sqrt{\text{total scan time}}} \quad [6]$$

Conventionally, a reduction in bSSFP banding is accompanied by a loss in SNR efficiency from multiple-acquisition bSSFP combination techniques, due to lengthened total scan time. However, using the proposed phase-cycled CAIPI-SMS bSSFP technique, there is minimal loss in SNR efficiency besides the potential g-factor penalty induced by the SMS acquisition.

Results

Simulations

The effect of the number of ramp-up preparation pulses on the bSSFP signal behavior is illustrated in Fig. 2. As shown in Fig. 2(b), 48 ramp-up pulses clearly yield improved stabilization of the bSSFP signal with reduced oscillations in $2\pi/3$ shifted signal curves, as compared to those with 24 ramp-up pulses presented in Fig. 2(a). The implication is that a longer ramp-up preparation pulse train is required to stabilize the CAIPI-SMS bSSFP signal.

Phantom imaging

The aliased CAIPI-SMS slices from the gel phantom were unfolded, resulting in multiple phase-cycled images as shown in Fig. 3(a). Images collected at the same slice position using

the single-band phase-cycled bSSFP were also displayed in Fig. 3(b). Overall, similar image quality and banding behavior are observed between CAIPI-SMS and the multiple-acquisition single-band bSSFP techniques. Notably, different phase cycling leads to variation in the banding behavior, e.g., shifts in banding location, reflecting the shifted off-resonance bSSFP profiles. As expected, the visual appearance in both maximum intensity and sum-of-square combined images show the least amount of residual banding with N=4 for both scenarios. These observations are further confirmed by the quantitative measurements presented in Fig. 4.

Phase cycling with N=4 offers the lowest percent ripple values, as shown in Fig. 4(a), for both maximum intensity and sum-of-square combined images. Quantified spatial SNR efficiency values are displayed in Fig. 4(b), where the highest SNR efficiency is attained with sum-of-square combined N=4 phase-cycled acquisition. The above findings were similarly observed from phase-cycled CAIPI-SMS and multiple-acquisition single-band bSSFP acquisitions. Further, the phase-cycled CAIPI-SMS bSSFP of scheme 3 outperforms its counterparts of scheme 1 and 2 and single-band techniques in terms of SNR efficiency.

In vivo brain imaging

Figure 5 shows the multiple phase-cycled un-aliased bSSFP images acquired on brain using interleaved CAIPI-SMS with temporally modulated phase cycling (scheme 3). The same imaging slices were acquired with different phase cycling, i.e., MB-2 with FOV/2 shift (top), MB-3 with FOV/3 shift (middle) and MB-4 with FOV/4 shift (bottom). Similar to results from the phantom study, different phase cycling leads to drastic variation in the location of the banding artifacts. Maximum intensity and sum-of-squares combined images indicate that banding artifacts are suppressed effectively in all scenarios. Visually, the least amount of residual banding artifact is seen in the MB-4 case. Hence, the performance of banding reduction improves as the number of phase cycling or SMS acceleration factor increases. These observations were further confirmed by the quantitative evaluation of the percent ripple, as indicated in Table 1. In this case, sum-of-square outperforms the maximum intensity combination scheme because of the overall lower ripple and higher SNR efficiency measurements.

Figure 6 shows the effect of ramp-up preparation pulses on banding reduction. Combined bSSFP images acquired with 24 and 48 ramp-up pulses are demonstrated in Fig. 6(a) and (b), respectively. As shown in the zoomed region, combined image with fewer ramp up pulses are prone to more pronounced residual banding, as well as the ripple artifact caused by the residual bSSFP signal oscillations.

Figure 7 demonstrates the capability of the CAIPI-SMS for whole-brain multi-slice banding-free bSSFP imaging. The CAIPI-SMS bSSFP scans with an acceleration factor of 4 and the single-band bSSFP are shown in Fig. 7(a) and (b), respectively. Within the same imaging time, the banding artifact is effectively removed in the latter case.

In vivo body imaging

Phase-cycled bSSFP imaging acquired with the CAIPI-SMS technique with an acceleration factor of 3 is demonstrated for abdominal and heart in Fig. 8 and 9, respectively. Three

aliased slices were successfully unfolded, and further combined to reduce the banding artifacts. Due to the large FOV in abdominal imaging, multiple banding artifacts appeared in the individual phase-cycled images, especially near the ribcage and within the abdominal cavity (arrows). The banding artifacts were effectively suppressed in the maximum intensity and sum-of-square combined images (Fig. 8). For cardiac imaging, banding artifacts also appeared in individual phase-cycled images either near or in the myocardium (arrows), which are suppressed in the combined images (Fig. 9). There is also artifact introduced by the flowing spins in the presence of off-resonance in bSSFP imaging (e.g. 2nd phase of slice 3 in Fig. 9). These flow related artifacts cannot be completed removed but are largely suppressed in the combined images.

Discussions

In this work, a novel approach for time-efficient bSSFP banding reduction by utilizing CAIPI-SMS imaging is presented. This technique exploits the inherent phase modulation of CAIPIRINHA to acquire multiple phase-cycled bSSFP images. The imaging time of CAIPI-SMS bSSFP is the same as that of a single-band bSSFP scan, however the amount of imaging data acquired is multiplied by the SMS slice acceleration factor which matches the number of phase cycling required for banding reduction. In the present study, we employed two common signal combination algorithms — maximum intensity and sum of squares, which showed promising results for banding reduction on brain, abdominal and cardiac imaging. The performance of the proposed technique is expected to be further improved with more advanced algorithms for recovering signal voids from phase-cycled images (12). In the present study, we also noticed that the image contrast and signal intensity vary across different phase-cycled bSSFP images due to the shifted off-resonance profile (see Fig. 9). However, the combined images not only show reduced banding but also stable contrast between tissues. This may facilitate clinical diagnosis and comparison of bSSFP images across time.

In SMS imaging with CAIPIRINHA, coil sensitivity variations along both slice and phase encoding directions are utilized (14). With the increasing availability of high-density phased array RF coils, SMS imaging has drawn growing research interest in the past few years (16,17). In the present study, we demonstrated that the presented technique can be applied in brain imaging for efficient banding reduction using a 32-channel head coil. Potential applications of the proposed CAIPI-SMS bSSFP technique for brain imaging include SSFP based fMRI (7), MR angiography (MRA) and cerebrospinal fluid (CSF) imaging (6,23). In addition, a proof-of-concept study was performed on the body with abdominal and cardiac imaging, where the presented methodology may find wider applications, e.g., cardiovascular MRI, where 2D multi-slice imaging has many advantages over 3D imaging and field inhomogeneity is more severe than that in the brain. Since phase-cycled CAIPI-SMS images are acquired consecutively in the proposed technique, motion between SMS acquisitions may present a challenge especially for cardiac and abdominal imaging. With the use of breath holding and cardiac triggering, we were able to effectively control motion for SMS bSSFP imaging of body organs without performing offline image registration (see supporting Fig. S1). Furthermore, non-rigid image registration algorithms can be applied to minimize the motion effects before combination of phase-cycled images (24). Overall, the

capability of acquiring multiple phase-cycled bSSFP images within a single scan is much more advantageous than performing multiple phase-cycled bSSFP scans, especially for body imaging.

In the present study, three schemes were proposed for the implementation of phase-cycled CAIPI-SMS bSSFP. Scheme 1 represents the most straightforward technical implementation, whereas scheme 2 and 3 involve temporally modulated phase cycling in conjunction with CAIPIRINHA SMS imaging. From quantitative phantom results shown in Fig. 4, the performance of scheme 1 and 2 are fairly comparable given the same *g*-factor for SMS imaging. Scheme 3 offers higher SNR efficiencies than the rest of the techniques since the MB inter-slice gap is larger for the interleaved acquisition. However, it is only suitable for covering a relatively large volume with a high density of imaging slices. Therefore, the three schemes of CAIPI-SMS bSSFP can be selectively applied for specific applications, and scheme 2 and 3 are preferred since they provide complete set of phase-cycled images for all slice positions. In this work, phase-cycled CAIPIRINHA shift was achieved by modulating the phases of the MB RF pulses. An alternative approach to achieve the CAIPIRINHA shift is to apply gradient blips in bSSFP imaging (25). The potential advantage of the gradient blip approach is that MB slices would be acquired without different shifts along the off-resonance profile, and phase cycling could be achieved in a conventional manner with similar benefits as described above. This could be an interesting topic for future work.

While the advantage of the presented technique is reduction in scan time as compared to the conventional phase cycling approach, specific absorption rate (SAR) of RF power increases with the MB factor. We have not encountered a SAR limit in our experiments which were carried out on 3T with a FA up to 51° and SMS factors up to 4. The potential SAR limit of CAIPI-SMS bSSFP can be addressed with advanced MB RF pulse design that offers reduced RF power deposition and peak power (26,27). Previous work (2) has shown that establishing steady state of bSSFP signal is more challenging in the presence of off-resonance effects, since the spin trajectory deviates from the simple oscillation around z. Similarly, since the simultaneously excited slices in SMS bSSFP imaging are acquired with shifted off-resonance profiles, it will take longer for SMS bSSFP signals to reach steady state compared to standard bSSFP imaging. As demonstrated by both simulation and *in vivo* experiments, a longer ramp-up pulse train is required for the proposed CAIPI-SMS bSSFP technique. Future work is required to develop more efficient magnetization preparation for CAIPI-SMS bSSFP.

The proposed SMS bSSFP technique could be sensitive to eddy currents induced by varying phase encoding gradients (28), given its requirement for accurate phase modulation with CAIPIRINHA. In the present study, eddy current has not caused major artifact possibly due to the linear *k*-space trajectory, which has small variation between consecutive encoding steps. For alternative encoding schemes such as golden angle radial trajectories or segmented phase encoding ordering for cardiac imaging, eddy currents may pose a challenge for SMS bSSFP imaging.

Conclusions

We introduced a novel approach for efficient banding reduction in bSSFP using phase-cycled CAIPI-SMS imaging. The advantage of the proposed technique is the reduction in scan time as compared to conventional phase cycling approach. Phase-cycled CAIPI-SMS bSSFP images from the brain and body organs demonstrate the feasibility and effectiveness of the proposed approach for banding reduction.

Supplementary Material

Refer to Web version on PubMed Central for supplementary material.

Acknowledgments

This research was supported by the National Institute of Health (NIH) Grants R01-MH080892, R01-NS081077, R01-EB014922, the NIH Human Connectome Project (NIH U54MH091657), Biomedical Technology Resource Centers (BTRC) National Center for Research Resources (NCRR; P41 RR08079), the National Institute of Biomedical Imaging and Bioengineering (NIBIB; P41 EB015894) and Siemens Healthcare USA, Inc. The authors would like to thank the two reviewers for valuable suggestions as well as Fei Han and Da Wang for their assistance in cardiac imaging.

References

1. Carr HY. Steady-State Free Precession in Nuclear Magnetic Resonance. Physical Review Letters. 1958; 1(11):429–430.
2. Scheffler K, Lehnhardt S. Principles and applications of balanced SSFP techniques. European radiology. 2003; 13(11):2409–2418. [PubMed: 12928954]
3. Zur Y, Stokar S, Bendel P. An analysis of fast imaging sequences with steady-state transverse magnetization refocusing. Magn Reson Med. 1988; 6(2):175–193. [PubMed: 3367775]
4. Peters DC, Ennis DB, McVeigh ER. High-resolution MRI of cardiac function with projection reconstruction and steady-state free precession. Magn Reson Med. 2002; 48(1):82–88. [PubMed: 12111934]
5. Peng Q, McColl RW, Wang J, Chia JM, Weatherall PT. Water-saturated three-dimensional balanced steady-state free precession for fast abdominal fat quantification. J Magn Reson Imaging. 2005; 21(3):263–271. [PubMed: 15723372]
6. Bangerter NK, Cukur T, Hargreaves BA, Hu BS, Brittain JH, Park D, Gold GE, Nishimura DG. Three-dimensional fluid-suppressed T2-prep flow-independent peripheral angiography using balanced SSFP. Magn Reson Imaging. 2011; 29(8):1119–1124. [PubMed: 21705166]
7. Lee J, Shahram M, Schwartzman A, Pauly JM. Complex data analysis in high-resolution SSFP fMRI. Magn Reson Med. 2007; 57(5):905–917. [PubMed: 17457883]
8. Gold GE, Hargreaves BA, Reeder SB, Block WF, Kijowski R, Vasanawala SS, Kornaat PR, Bammer R, Newbould R, Bangerter NK, Beaulieu CF. Balanced SSFP imaging of the musculoskeletal system. J Magn Reson Imaging. 2007; 25(2):270–278. [PubMed: 17260387]
9. Bangerter NK, Hargreaves BA, Vasanawala SS, Pauly JM, Gold GE, Nishimura DG. Analysis of multiple-acquisition SSFP. Magn Reson Med. 2004; 51(5):1038–1047. [PubMed: 15122688]
10. Cukur T, Lustig M, Nishimura DG. Multiple-profile homogeneous image combination: application to phase-cycled SSFP and multicoil imaging. Magn Reson Med. 2008; 60(3):732–738. [PubMed: 18727089]
11. Quist B, Hargreaves BA, Daniel BL, Saranathan M. Balanced SSFP Dixon imaging with banding-artifact reduction at 3 Tesla. Magn Reson Med. 2015; 74(3):706–715. [PubMed: 25227766]
12. Xiang QS, Hoff MN. Banding artifact removal for bSSFP imaging with an elliptical signal model. Magn Reson Med. 2014; 71(3):927–933. [PubMed: 24436006]

13. Benkert T, Ehses P, Blaimer M, Jakob PM, Breuer FA. Dynamically Phase-Cycled Radial Balanced SSFP Imaging for Efficient Banding Removal. Magn Reson Med. 2015; 73(1):182–194. [PubMed: 24478187]
14. Blaimer M, Choli M, Jakob PM, Griswold MA, Breuer FA. Multiband Phase-Constrained Parallel MRI. Magn Reson Med. 2013; 69(4):974–980. [PubMed: 23440994]
15. Stab D, Ritter CO, Breuer FA, Weng AM, Hahn D, Kostler H. Caipirinha Accelerated Ssfp Imaging. Magn Reson Med. 2011; 65(1):157–164. [PubMed: 20872868]
16. Larkman DJ, Hajnal JV, Herlihy AH, Coutts GA, Young IR, Ehnholm G. Use of multicoil arrays for separation of signal from multiple slices simultaneously excited. Journal of Magnetic Resonance Imaging. 2001; 13(2):313–317. [PubMed: 11169840]
17. Moeller S, Yacoub E, Olman CA, Auerbach E, Strupp J, Harel N, Ugurbil K. Multiband Multislice GE-EPI at 7 Tesla, With 16-Fold Acceleration Using Partial Parallel Imaging With Application to High Spatial and Temporal Whole-Brain FMRI. Magn Reson Med. 2010; 63(5):1144–1153. [PubMed: 20432285]
18. Breuer FA, Blaimer M, Heidemann RM, Mueller MF, Griswold MA, Jakob PM. Controlled aliasing in parallel imaging results in higher acceleration (CAIPIRINHA) for multi-slice imaging. Magn Reson Med. 2005; 53(3):684–691. [PubMed: 15723404]
19. Friedman L, Glover GH. Report on a multicenter fMRI quality assurance protocol. J Magn Reson Imaging. 2006; 23(6):827–839. [PubMed: 16649196]
20. Setsompop K, Gagoski BA, Polimeni JR, Witzel T, Wedeen VJ, Wald LL. Blipped-controlled aliasing in parallel imaging for simultaneous multislice echo planar imaging with reduced g-factor penalty. Magn Reson Med. 2012; 67(5):1210–1224. [PubMed: 21858868]
21. Wang Y, Moeller S, Li X, Vu AT, Krasileva K, Ugurbil K, Yacoub E, Wang DJ. Simultaneous multi-slice Turbo-FLASH imaging with CAIPIRINHA for whole brain distortion-free pseudo-continuous arterial spin labeling at 3 and 7T. NeuroImage. 2015; 113:279–288. [PubMed: 25837601]
22. Parker DL, Gullberg GT. Signal-to-noise efficiency in magnetic resonance imaging. Med Phys. 1990; 17(2):250–257. [PubMed: 2333051]
23. Jolesz FA, Patz S, Hawkes RC, Lopez I. Fast imaging of CSF flow/motion patterns using steady-state free precession (SSFP). Investigative radiology. 1987; 22(10):761–771. [PubMed: 3429171]
24. Wang DJ, Bi X, Avants BB, Meng T, Zuehlsdorff S, Detre JA. Estimation of perfusion and arterial transit time in myocardium using free-breathing myocardial arterial spin labeling with navigator-echo. Magn Reson Med. 2010; 64(5):1289–1295. [PubMed: 20865753]
25. Duerk, J.; Griswold, M.; Dara, K. Case Western Reserve University, assignee. Multi-slice blipped TRUEFISP-CAIPIRINHA. patent US 20130271128A1. 2013 Oct 17. 2013
26. Norris DG, Koopmans PJ, Boyacioglu R, Barth M. Power Independent of Number of Slices (PINS) radiofrequency pulses for low-power simultaneous multislice excitation. Magn Reson Med. 2011; 66(5):1234–1240. [PubMed: 22009706]
27. Wong, E. Proc of the 20th Annual Meeting of ISMRM. Melbourne, Australia: 2012. Optimized phase schedules for minimizing peak RF power in simultaneous multi-slice RF excitation pulses; p. 2209
28. Bieri O, Markl M, Scheffler K. Analysis and compensation of eddy currents in balanced SSFP. Magn Reson Med. 2005; 54(1):129–137. [PubMed: 15968648]

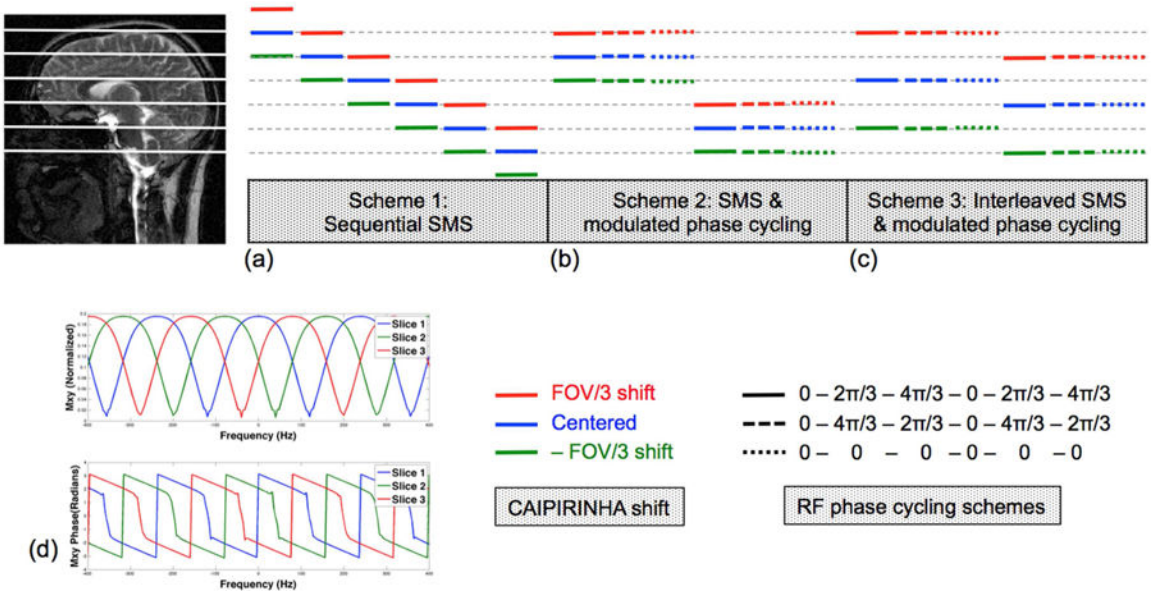

Figure 1.

Schematic diagram of the phase-cycled MB-3 bSSFP acquisition and the corresponding off-resonance profile. (a-c) Different schemes to achieve phase-cycled CAIPI-SMS bSSFP imaging. Each set of red, blue and green lines represent three slices that are excited and readout simultaneously. Solid and dashed lines represent modulated phase-cycled bSSFP acquisitions. (d) Magnitude (top) and phase (bottom) of bSSFP off-resonance profile. Specifically, red, blue and green represent slices with a FOV/3, centered and - FOV/3 shift along the phase encoding direction, or $2\pi/3$, 0, $-2\pi/3$ shift in their off-resonance profiles.

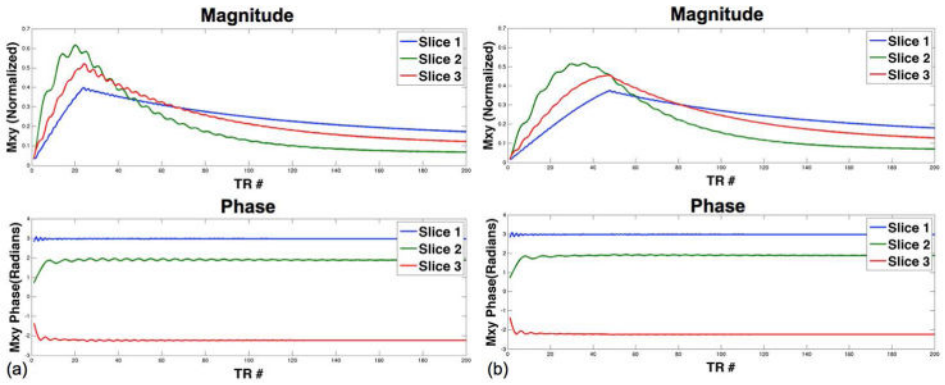

Figure 2.

Simulated magnitude (top) and phase (bottom) of the MB-3 bSSFP signal with (a) 24 and (b) 48 ramp-up preparation pulses. Red, blue and green slices match the color scheme used in Fig. 1.

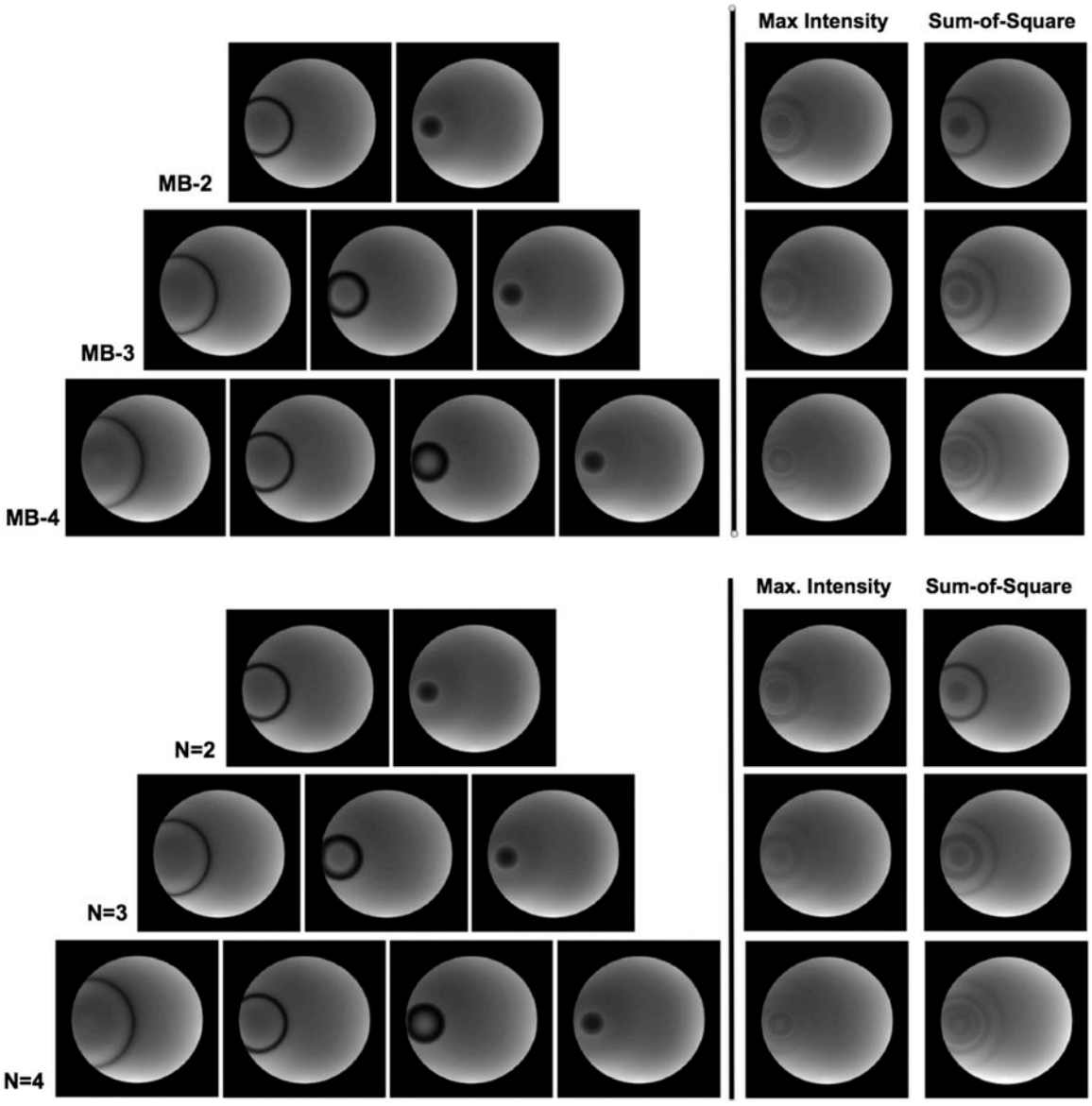

Figure 3.

Example un-aliased individual phase-cycled images acquired using (a) CAIPI-SMS bSSFP with scheme 3 and (b) single-band bSSFP. *N*=2 (top), 3 (middle) and 4 (bottom) phase cycling are shown. The location of banding artifacts shifts between different phase cycling. The composite images are generated by maximum intensity and sum-of-squares combination schemes.

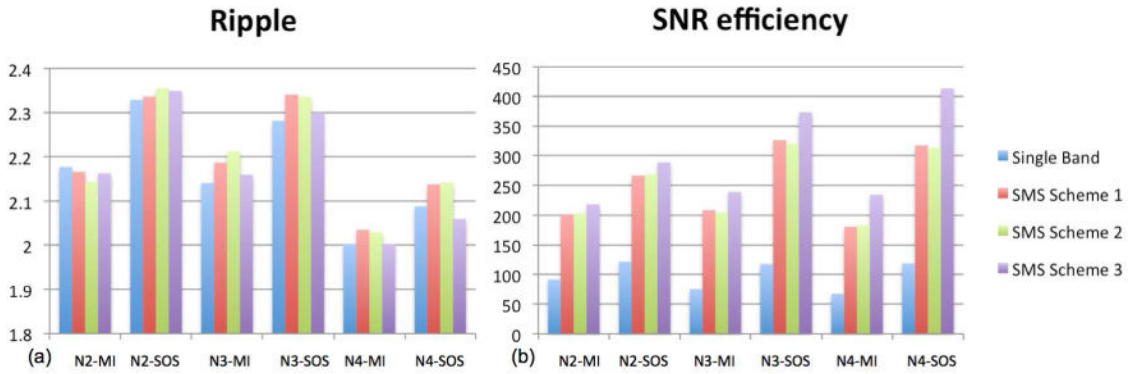

Figure 4.

Quantitative analysis of phase-cycled SMS bSSFP and single-band phase-cycled bSSFP. (a) Percent ripple, and (b) SNR efficiency from the banding affected region.

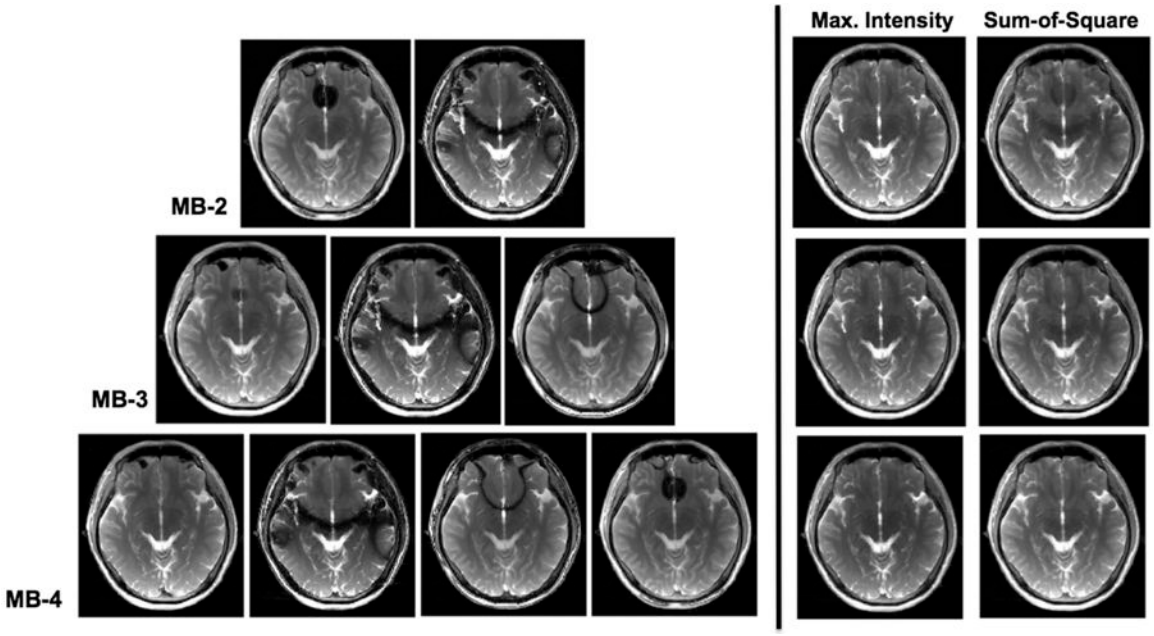

Figure 5.

Un-aliased individual phase-cycled axial slices of the brain acquired using interleaved CAIPI-SMS bSSFP with modulated phase cycling (scheme 3). The location of banding artifacts shifts between different phase cycling. Composite images generated by maximum intensity (left) and sum-of-squares (right) image combination at MB-2 (top), MB-3 (middle) and MB-4 (bottom) acceleration are shown.

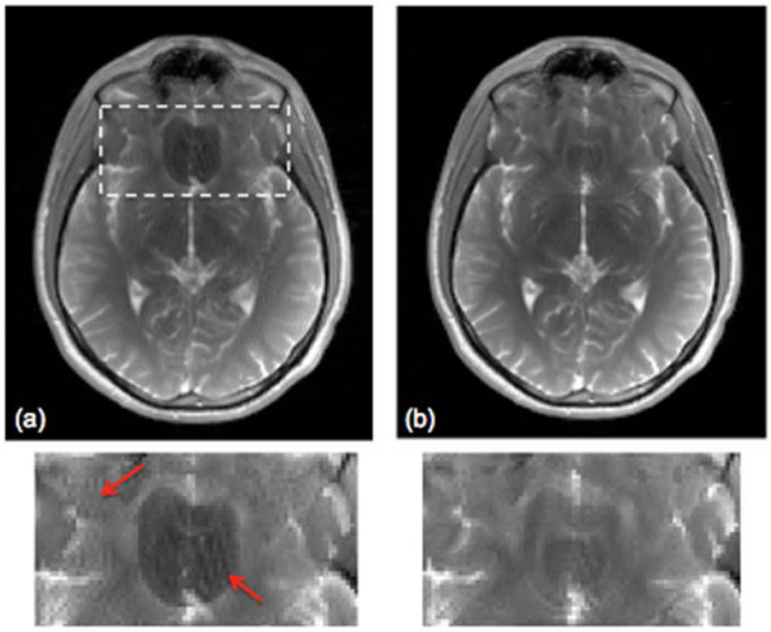

Figure 6.

The effect of ramp up preparation pulses on multiple acquisition combined bSSFP images. Maximum intensity combined images based on a CAIPI-SMS scan with acceleration factor of 3 and a FOV/3 in-plane shift. (a) 24 and (b) 48 ramp-up preparation pulses.

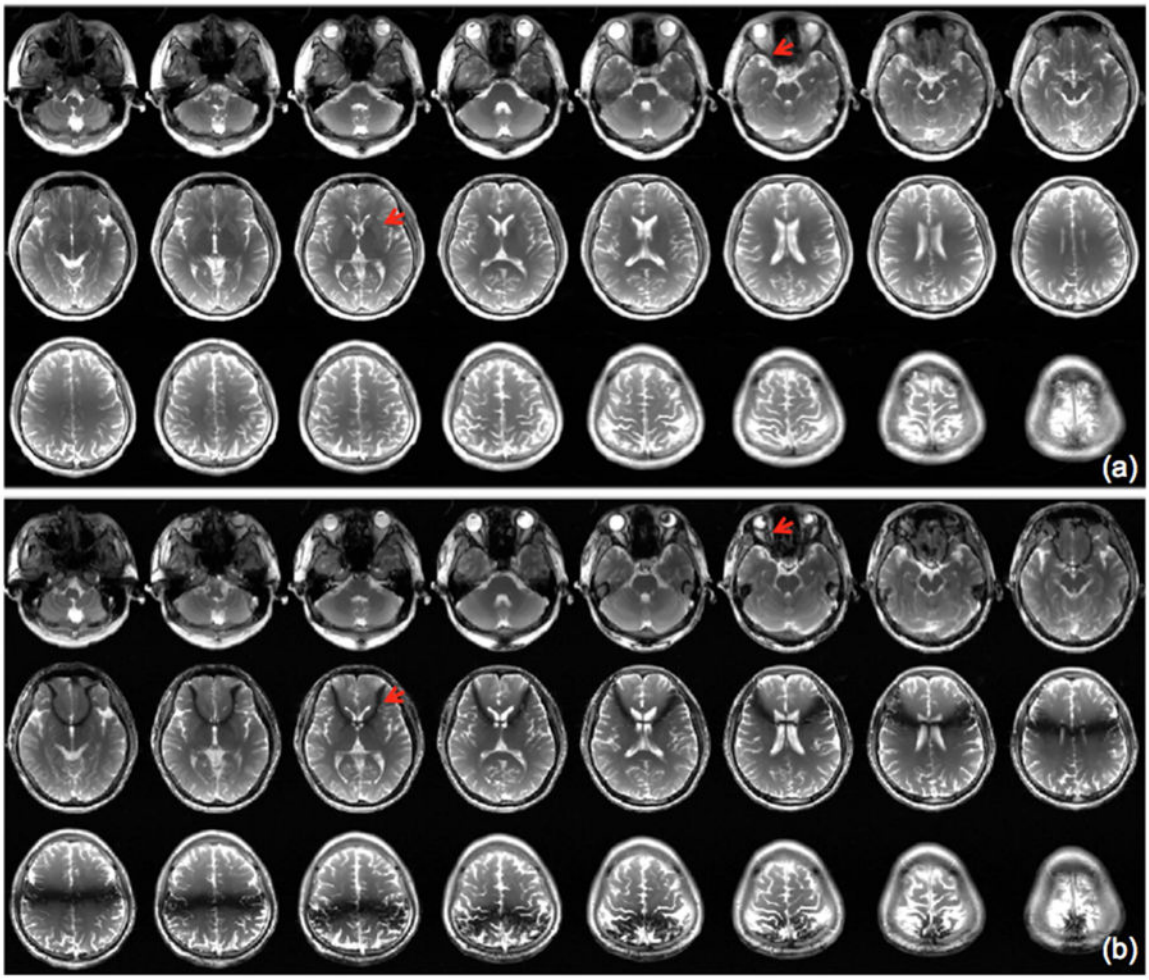

Figure 7.

Whole brain bSSFP images acquired with (a) interleaved CAIPI-SMS bSSFP with a SMS factor of 4 and a FOV/4 shift, and (b) single-band bSSFP. Banding artifacts in the standard bSSFP images (red arrows) are completely removed in the CAIPI-SMS combined images at the corresponding locations.

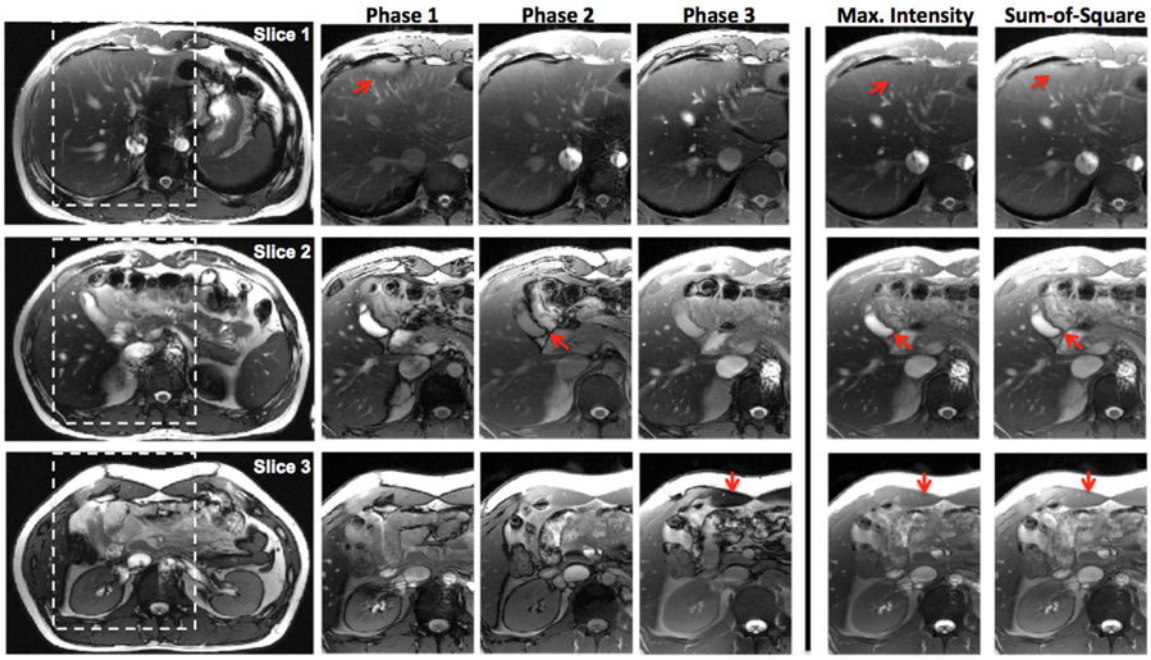

Figure 8.
CAIPI-SMS bSSFP with MB-3 for abdominal imaging. Unfolded individual phase-cycled images and the combined images with magnified views are shown.

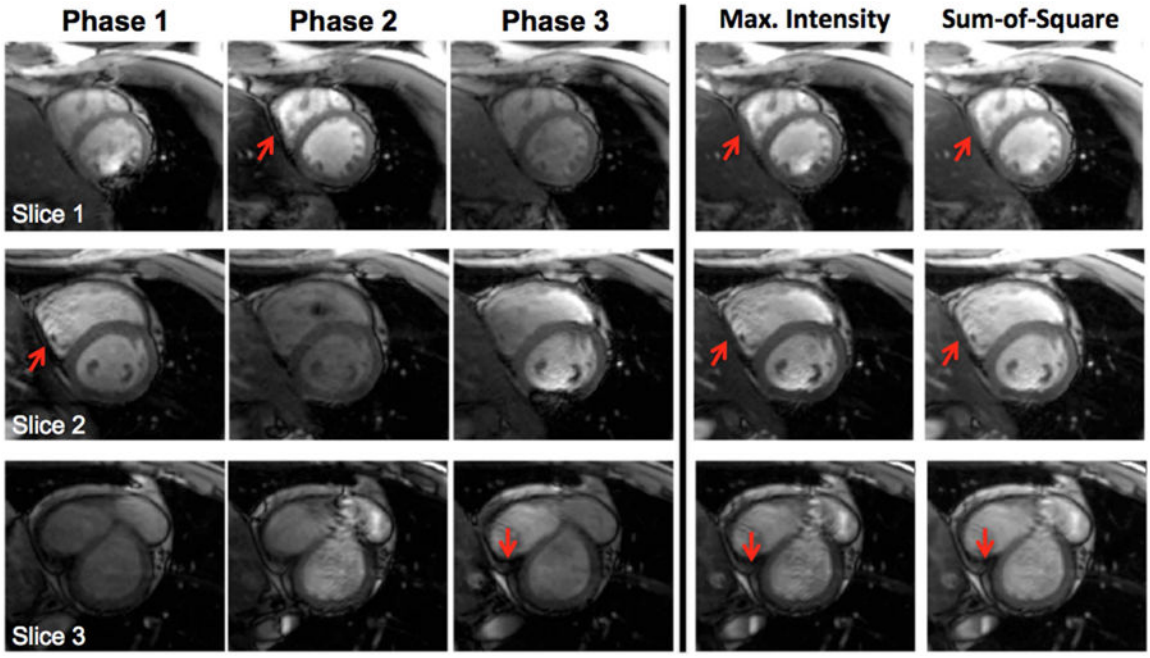

Figure 9.

Enlarged sections of three short axis cardiac bSSFP images, acquired using CAIPI-SMS bSSFP with a MB factor of 3 and a FOV/3 CAIPIRINHA shift. Unfolded individual phase-cycled images and the combined images are shown.

Table 1

Quantitative analysis of the interleaved CAIPI-SMS bSSFP imaging with modulated phase cycling (scheme 3) for brain imaging. The sum-of-square outperforms the maximum intensity combination schemes with overall lower ripple and higher spatial SNR efficiencies.

Quantitative analysis	Max. Intensity			Sum-of-Square		
	MB=2	MB=3	MB=4	MB=2	MB=3	MB=4
Ripple	4.07±0.93	4.39±0.31	4.15±0.47	3.59±0.74	3.40±0.10	3.20±0.13
SNR efficiency	41.42±21.07	42.41±19.52	43.16±15.20	53.35±26.91	63.65±30.09	73.37±26.31